ЖЭТФ, 2007, том 132, вып. 3 (9), стр. 666–672

NONFRUSTRATED MAGNETOELECTRIC WITH INCOMMENSURATE MAGNETIC ORDER IN THE MAGNETIC FIELD

A. V. Syromyatnikov*

St. Petersburg Nuclear Physics Institute
188300, Gatchina, St. Petersburg, Russia

Received February 19, 2007

We discuss a model nonfrustrated magnetoelectric in which a sufficiently strong magnetoelectric coupling produces an incommensurate magnetic order leading to ferroelectricity. Properties of the magnetoelectric in the magnetic field directed perpendicular to the wave vector describing the spin helix are considered in detail. Analysis of the classical energy shows that in contrast to the naive expectation, the onset of ferroelectricity occurs at a field H_{c1} that is lower than the saturation field H_{c2}. We have $H_{c1} = H_{c2}$ at large enough magnetoelrctric coupling. We show that at $H = 0$, ferroelectricity occurs at $T = T_{FE} < T_N$. A qualitative discussion of the phase diagram in the $H - T$ plane is presented within the mean-field approach.

PACS: 75.80.+q, 71.70.Ej, 77.80.-e

1. INTRODUCTION

In recent years, there has been a revival of interest in magnetic ferroelectrics in which magnetic and ferroelectric orders coexist (magnetoelectrics) [1, 2]. Systems in which the ferroelectric and spiral magnetic order occur simultaneously attract particular attention presently because of the recognition of the role that such materials might play in fabricating novel magnetoelectric (ME) devices [3]. A number of such compounds have been obtained recently: $RMnO_3$ with R = Gd, Tb, Dy [4–6]; RMn_2O_5 with R = Ho, Y, Tb, Dy [7–9]; $Ni_3V_2O_8$ [10, 11]; spinel oxides RCr_2O_4 with R = Co, Fe, Mn [12]; $MnWO_4$ [13] etc. In the majority of these materials, the paraelectric phase with a collinear spin structure (sinusoidal spin density wave) appears below the Néel temperature T_N. Upon further cooling, at $T = T_{FE} < T_N$, a transition occurs to the phase in which the ferroelectric order coexists with an incommensurate elliptical (conical in RCr_2O_4) magnetic spiral. Some of such ferroelectric phases (e.g., $RMnO_3$ and RCr_2O_4) are stable down to very small temperatures; in others, transitions to collinear paraelectric phases occur below T_{FE}. All experiments point to the key role of the noncollinear spin configurations induced by frustrated exchange interactions in producing the electric polarization [2]. Due to the frustration, T_N and T_{FE} are quite small in all compounds found by now, with only one exception, $Ba_{0.5}Sr_{1.5}Zn_2Fe_{12}O_{22}$ [14], in which T_{FE} is greater than room temperature. A "giant" ME effect is observed in these materials as a very high sensitivity of the electric polarization to the magnetic field: the spin-flop transition in the magnetic field is accompanied by rotation of the polarization through 90° and by an anomaly in the dielectric constant. The value of the electric polarization was found to be two to three orders smaller than in the typical ferroelectrics; there is no such great influence of the electric field on the magnetic properties, which indicates that the ME coupling is small in these compounds. Much effort has been invested in finding materials with a stronger ME coupling and with higher transition temperatures, which can be used in practice.

A phenomenological treatment of the magnetoelectric coupling mechanism has been proposed based on the Landau expansion and symmetry considerations [3, 15–17]. A microscopic mechanism of ferroelectricity of the magnetic origin was recently proposed in Ref. [18], based on the idea that the spin current $\mathbf{j}_s \propto [\mathbf{S}_i \times \mathbf{S}_j]$ induced between the noncollinear spins leads to the electric moment $\mathbf{P} \propto [\mathbf{e}_{ij} \times \mathbf{j}_s]$, where $\mathbf{e}_{ij}$

*E-mail: syromyat@thd.pnpi.spb.ru

is the unit vector connecting spins i and j. This result can be regarded as the inverse effect of the Dzyaloshinskii–Moriya interaction. As a result, the effective ME interaction can be writen as [19]

$$V_{ME} = \beta[\mathbf{U} \times \mathbf{e}_{ij}] \cdot [\mathbf{S}_i \times \mathbf{S}_j], \qquad (1)$$

where $\mathbf{U}$ stands for the corresponding ligand displacement. Taking the elastic energy $\gamma U^2/2$ into account shows that the proposed mechanism can lead to ferroelectricity as soon as the noncollinear spin structure exists.

The ME coupling in (1) can produce a spiral incommensurate magnetic order and electric moment even without frustration if β is large enough. Indeed, we consider two spins and take the direct exchange coupling J between them, ME interaction (1), and the elastic energy $\gamma U^2/2$ into account. Minimization of the total energy with respect to U and ϕ, the angle between the spins, gives $U = (\beta/\gamma)S^2 \sin\phi$ and $\sin\phi\cos\phi = \gamma J/(\beta S)^2 \sin\phi$. The ME coupling constant in $TbMnO_3$, currently one of the best magnetoelectrics of this type, is estimated to be $\beta \sim 1$ meV/Å [17]. With the characteristic value of γ given by 10^3 meV/Å^2 and $J \sim 1$ meV, it follows from the above estimates that $\sin\phi\cos\phi \approx 10^3 \sin\phi$, which leads to $\phi = 0$ and indicates that in magnetoelectric compounds that have been found presently, frustration is indeed indispensable for the appearance of a noncollinear magnetic order leading to ferroelectricity. As mentioned above, every effort is now made to find incommensurate magnetoelectrics with a larger ferroelectric moment. But the strong ME interaction can produce a spiral incommensurate magnetic order and a ferroelectric moment without frustration. Thus, it can be seen from the above consideration of two spins that if β were about 30 times larger than in $TbMnO_3$, a nonzero solution for ϕ would appear. Moreover, it can be expected that among the magnetoelectric compounds with large enough β to be obtained (as we hope), nonfrustrated compounds would have larger transition temperatures than frustrated ones, other things being equal.

Thus, it is instructive to discuss nonfrustrated magnets with a strong ME coupling of form (1). Such a magnet was recently considered in Ref. [19], where collective magnetoelectric modes were discussed. In the present paper, we discuss a model similar to that in Ref. [19], focusing on its properties in the magnetic field directed perpendicular to wave vector describing the spin helix. Analysis of the classical energy presented in Sec. 2 shows that in contrast to the naive expectation, the onset of ferroelectricity occurs at a field H_{c1} that is lower than the saturation field H_{c2}. We have $H_{c1} = H_{c2}$ at strong enough β. We show that at $H = 0$, ferroelectricity occurs at $T = T_{FE} < T_N$. A qualitative discussion of the phase diagram in the $H-T$ plane is presented within the mean-field approach in Sec. 3. Section 4 contains our conclusions.

2. CLASSICAL ENERGY

We discuss a magnetoelectric with the ferromagnetic interaction J_{ij}^{xy} in the xy plane and the antiferromagnetic interaction J_{ij}^{z} along the z axis with the ME coupling of form (1). The corresponding Hamiltonian has the form

$$\mathcal{H} = \frac{1}{2}\sum_{(i,j)} J_{ij}^z \mathbf{S}_i\mathbf{S}_j - \frac{1}{2}\sum_{\langle i,j\rangle} J_{ij}^{xy}\mathbf{S}_i\mathbf{S}_j + \beta\sum_i [\mathbf{U}_{\mathbf{R}_i} \times \mathbf{e}_x] \cdot [\mathbf{S}_{\mathbf{R}_i} \times \mathbf{S}_{\mathbf{R}_i+\mathbf{e}_x}] + \frac{\gamma}{2}\sum_i U_i^2 + H\sum_i S_i^z, \qquad (2)$$

where (i,j) and $\langle i,j\rangle$ respectively denote nearest neighbors along the z axis and in the xy plane, $\mathbf{e}_x$ is the unit vector along the x axis, the lattice constant is taken to be equal to unity, β and γ are positive constants, and the last term is the Zeeman energy in the field directed along the z axis (see Fig. 1). At $H = 0$, spins lie in the xy plane and their rotation is described by the wave vector $\mathbf{q} = (q, 0, 0)$. There is a uniform displacement $\mathbf{U}_i = \mathbf{U} = (0, U, 0)$ along the y axis. The electric polarization of the sample $\mathbf{P}$ is proportional to $N\mathbf{U}$, where N is the number of spins in the lattice. When $H \neq 0$, the spins cant in the direction opposite to the field direction and make an angle $\theta < \pi/2$ with the z axis (see Fig. 1). Magnetoelectrics with the ferromagnetic exchange along the z axis or the antiferromagnetic exchange in the xy plane can be considered on equal footing. We discuss the corresponding results qualitatively in Sec. 4.

To find q, U, and θ, we must minimize the classical energy with respect to U, q, and θ. The classical energy is given by

$$\frac{E}{N} = 2J^zS^2\cos^2\theta - J^{xy}S^2(\cos^2\theta + \sin^2\theta\cos q) - \beta S^2 U \sin^2\theta \sin q + \frac{\gamma}{2}U^2 - HS\cos\theta, \qquad (3)$$

where S is the spin value. The equations for the minimum of Eq. (3) have two solutions: (i) that with a collinear spin structure, $q = U = 0$, and (ii) that with

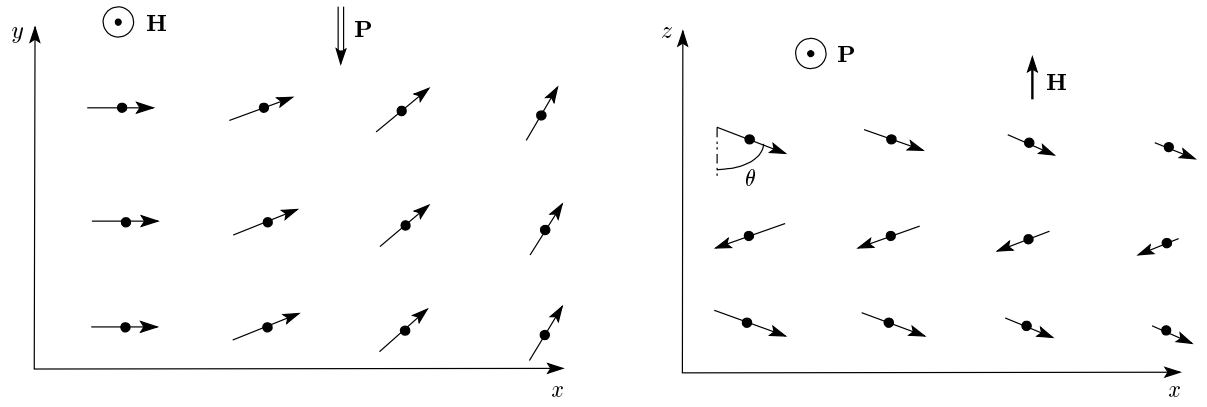

Fig. 1. Projections of spins on xy and xz planes are shown in the noncollinear phase of the magnetoelectric discussed. The magnetic field $\mathbf{H}$, the electric polarization $\mathbf{P}$, and the canting angle θ of spins in the magnetic field are shown

a spiral spin structure, $q \neq 0$ and $U \neq 0$. The last solution is given by

$$U = \frac{\beta S^2}{\gamma} \sin^2\theta \sin q, \tag{4a}$$

$$j_{xy} = \cos q \sin^2\theta, \tag{4b}$$

$$H = \frac{2\beta^2 S^3}{\gamma} \cos\theta \left(\sin^2\theta + 2j_z - j_{xy}\right), \tag{4c}$$

where two dimensionless constants are introduced as

$$j_{xy} = \frac{\gamma J^{xy}}{(\beta S)^2}, \quad j_z = \frac{\gamma J^z}{(\beta S)^2}. \tag{5}$$

Stability conditions of the solutions are determined from the requirement of positive definiteness of the bilinear form $\partial^2 E/(\partial x \partial y)$, where $x, y = U, q, \theta$. In particular, the stability criteria of (4) are given by

$$q \neq 0, \tag{6a}$$

$$\cos\theta < \sqrt{\frac{1 - j_{xy} + 2j_z}{3}}. \tag{6b}$$

It can be seen from Eq. (4b) that this solution exists if

$$j_{xy} < 1. \tag{7}$$

We assume below that condition (7) holds. The other solution of Eq. (3) gives the collinear spin structure

$$U = q = 0, \tag{8a}$$

$$\cos\theta = \begin{cases} H/H_{c2}, & H \leq H_{c2}, \\ 1, & H > H_{c2}, \end{cases} \tag{8b}$$

where $H_{c2} = 4SJ^z$. Solution (8) is stable at sufficiently large fields, such that the condition

$$\cos\theta > \sqrt{1 - j_{xy}} \tag{9}$$

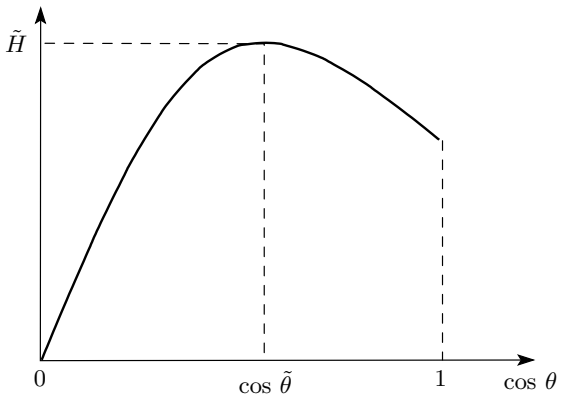

Fig. 2. Plot of the right-hand side of Eq. (4c) as a function of $\cos\theta$. Values of $\tilde{H}$ and $\tilde{\theta}$ are given by Eqs. (13) and (12), respectively

is satisfied. We conclude from Eqs. (7) and (9) that if (7) does not hold, only the collinear spin structure exists. In contrast, when (7) is satisfied, the collinear solution is stable only at $H > H_{c1}^{so}$, where

$$H_{c1}^{so} = 4SJ^z\sqrt{1 - j_{xy}}, \tag{10}$$

which is found using Eq. (8b) and assuming the equality in Eq. (9). The angle θ_{c1}^{so} corresponding to the field H_{c1}^{so} is given by

$$\cos\theta_{c1}^{so} = \sqrt{1 - j_{xy}}. \tag{11}$$

We note that Eq. (4b) gives $q = 0$ at $\theta = \theta_{c1}^{so}$.

We now turn to the transition between the spiral and collinear configurations. At $H = 0$ and $\theta = \pi/2$, the spiral configuration is realized. As is clear from Eq. (4c), the angle θ is an ambiguous function of H. A

plot of the right-hand side of Eq. (4c) is presented in Fig. 2. It shows a maximum at $\theta = \tilde{\theta}$, where

$$\cos\tilde{\theta} = \sqrt{\frac{1 - j_{xy} + 2j_z}{3}}. \tag{12}$$

If the right-hand side of Eq. (12) is larger than unity, it follows that $\tilde{\theta} = 0$ in the consideration presented below and only the regime with $\theta > \tilde{\theta}$ remains. According to Eq. (6b), we should take the solutions of Eq. (4c) with $\theta > \tilde{\theta}$. The value of the magnetic field corresponding to the maximum in Fig. 2 is given by

$$\tilde{H} = \frac{4\beta^2 S^3}{\gamma}\left(\frac{1 + 2j_z - j_{xy}}{3}\right)^{3/2}. \tag{13}$$

It can be easily shown using Eqs. (10) and (13) and the Cauchy inequality that $\tilde{H} \geq H_{c1}^{so}$. Then, analysis shows that the type of the phase transition is determined by the value of the angle θ_{c1}^{so} at which inequality (9) turns into the equality. Two regimes are possible at which we have continuous and discontinuous transitions, respectively: $\theta_{c1}^{so} < \tilde{\theta}$ and $\theta_{c1}^{so} > \tilde{\theta}$. It can be easily shown using Eqs. (11) and (12) that $\theta_{c1}^{so} < (>)\tilde{\theta}$ is equivalent to $j_{xy} + j_z < (>)1$. We discuss these two regimes separately.

A. Continuous transition

The transition is continuous if $\theta_{c1}^{so} > \tilde{\theta}$, i.e., if

$$j_{xy} + j_z > 1. \tag{14}$$

The angle θ decreases as the field increases and the spiral solution turns into the collinear one at $H = H_{c1}^{so}$: q and U reduce gradually to zero as H approaches H_{c1}^{so} and θ approaches θ_{c1}^{so}; at $H = H_{c1}^{so}$, we have $\theta = \theta_{c1}^{so}$, $q = U = 0$, the stability criterion of spiral solution (6a) ceases to hold and collinear solution (8) becomes stable (criterion (9) begins to hold). All spins become parallel to the field direction at $H = H_{c2}$. As a result, we obtain the phase diagram shown in Fig. 3*a* corresponding to the line $T = 0$.

B. Discontinuous transition

The transition is discontinuous if $\theta_{c1}^{so} < \tilde{\theta}$, i.e., if

$$j_{xy} + j_z < 1. \tag{15}$$

This regime corresponds to a larger spin–lattice coupling (larger β) than that discussed above. In this case, the angle θ_{c1} cannot be reached gradually because, in particular, the spiral solution is unstable at $\theta < \tilde{\theta} > \theta_{c1}^{so}$. Therefore, the transition is of the first order in this case. When H reaches H_{c1}^{so}, q does not vanish and the spiral solution remains stable. At the same time, the collinear solution is also stable at $H > H_{c1}^{so}$, but the energy of the spiral solution is lower than that of the collinear one at $H = H_{c1}^{so}$. As the magnetic field is further increased, the ground state energies of these two solutions come together and the transition occurs when they become equal. The corresponding field can be greater or lower than H_{c2}. In the first case, all spins in the collinear phase are parallel to the field ($\theta_{c1}^{fo} = 0$); in the second case, $\theta_{c1}^{fo} \neq 0$ and all spins become parallel to each other at $H > H_{c2}$ only. In the second scenario, using Eqs. (3), (4), and (8), it is easy to find the critical field

$$H_{c1}^{fo} = 2SJ^z\frac{1 - j_{xy} + j_z}{\sqrt{j_z}}. \tag{16}$$

The transition is accompanied by a decrease in the angle θ, from θ_{c1}^{fo} given by

$$\cos\theta_{c1}^{fo} = \sqrt{j_z} \tag{17}$$

to θ_{c1}^{so} given by Eq. (11), and in the wave vector q of the spiral switches, from

$$\cos q_{c1}^{fo} = \frac{j_{xy}}{1 - j_z} \tag{18}$$

to $q = 0$. Then we are led to the part of the phase diagram in the $H-T$ plane shown in Fig. 3*b* corresponding to the line $T = 0$.

We obtain that $H_{c1}^{fo} < H_{c2}$ if

$$\sqrt{j_{xy}} + \sqrt{j_z} > 1. \tag{19}$$

If β is so large that this criterion does not hold, there is only one critical field H_c, and we are led to the line $T = 0$ on the phase diagram shown in Fig. 3*c*. The expression for H_c is quite complicated and we do not present it here.

We now discuss the phase diagrams at $T > 0$.

3. FINITE TEMPERATURES

We find the equation for the phase transition line between collinear and spiral phases within the mean-field approximation (MFA). The energy in (3) is a function of T. Working in the MFA, we assume that the spin value is reduced by thermal fluctuations,

$$S(T) = S\left(1 - \frac{T}{T_N}\right), \tag{20}$$

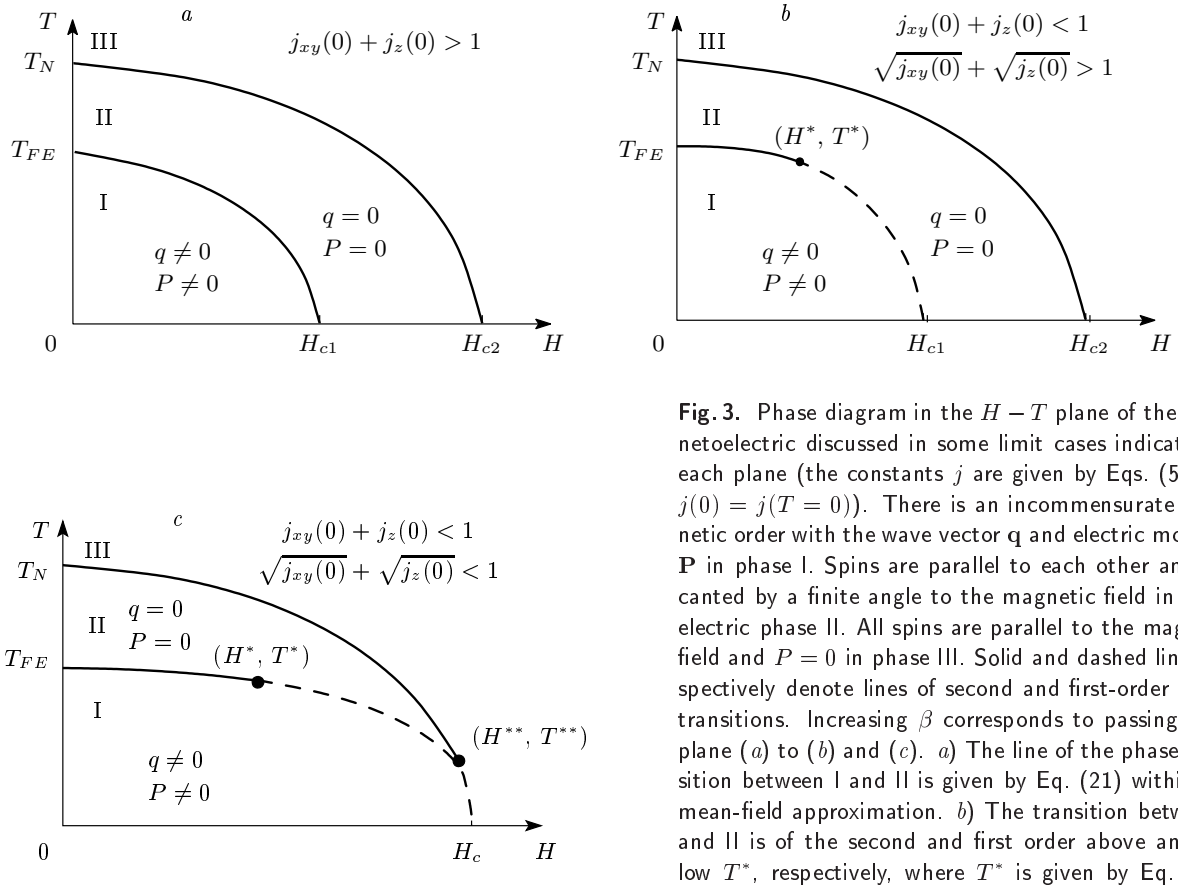

Fig. 3. Phase diagram in the $H-T$ plane of the magnetoelectric discussed in some limit cases indicated in each plane (the constants j are given by Eqs. (5) and $j(0)=j(T=0)$). There is an incommensurate magnetic order with the wave vector $\mathbf{q}$ and electric moment $\mathbf{P}$ in phase I. Spins are parallel to each other and are canted by a finite angle to the magnetic field in paraelectric phase II. All spins are parallel to the magnetic field and $P=0$ in phase III. Solid and dashed lines respectively denote lines of second and first-order phase transitions. Increasing β corresponds to passing from plane (*a*) to (*b*) and (*c*). *a*) The line of the phase transition between I and II is given by Eq. (21) within the mean-field approximation. *b*) The transition between I and II is of the second and first order above and below T^*, respectively, where T^* is given by Eq. (22). The line of phase transitions in this case is given within the MFA by Eqs. (21) and (23) above and below T^*, respectively. *c*) There is only one critical field H_c at $T=0$ in this regime. The temperatures T^* and T^{**} are given by Eqs. (22) and (24)

where $T_N=2S^2(J^z+2J^{xy})$ within the MFA, $S\gg 1$, and $T\ll T_N$. For simplicity, we neglect the dependence of the constants β, γ, and J on T in Eq. (3). As soon as the spin value depends on T, all S-dependent quantities occurring in the above discussion are also functions of T. In particular, using Eqs. (10) and (16), we can find the phase transition line in the $H-T$ plane between the spiral and collinear phases. This line is different in the case of the second-order and first-order phase transitions at $T=0$, i.e., at $j_{xy}(T=0)+j_z(T=0)>1$ and $j_{xy}(T=0)+j_z(T=0)<1$, which should be discussed separately.

A. Second-order phase transition at $T=0$ $(j_{xy}(T=0)+j_z(T=0)>1)$

Evidently, the phase transition line starting at $(H=0, T_N)$ must lead to the point $(H_{c2}, T=0)$. It is also clear that the phase transition line between the noncollinear and collinear phases must start at $(H_{c1}, 0)$ and end at $(0, T_{FE})$, where $T_{FE}<T_N$. Using Eqs. (10) and (20), we can easily find the equation for $H_{c1}^{so}(T)$:

$$\frac{T}{T_N}=\frac{[H_{c1}^{so}(0)]^2-[H_{c1}^{so}(T)]^2}{2(4SJ^z)^2}, \qquad (21)$$

which gives a parabola in the $H-T$ plane (see Fig. 3*a*). In particular, we have $T_{FE}=T_N[1-j_{xy}(0)]/2$ from Eq. (21). The requirement $T\ll T_N$ then implies that $j_{xy}(0)\sim 1$.

B. First-order phase transition at $T=0$ $(j_{xy}(T=0)+j_z(T=0)<1)$

The phase diagram is different depending on whether condition (19) holds at $T=0$.

1. $\sqrt{j_{xy}(0)} + \sqrt{j_z(0)} > 1$

It can be seen from Eqs. (5) that thermal fluctuations increase j_{xy} and j_z. Above a certain temperature T^*, the sum $j_{xy}(T) + j_z(T)$ then becomes larger than unity. Hence, at $T > T^*$ and $T < T^*$, where

$$T^* = T_N \frac{1 - j_{xy}(0) - j_z(0)}{2} \tag{22}$$

is found from the condition $j_{xy}(T^*) + j_z(T^*) = 1$, the transition is of the second and first order, respectively. The second-order phase transition line at $T > T^*$ is given by Eq. (21). The first-order phase transition line at $T < T^*$ can be found using Eq. (16), with the result

$$\frac{T}{T_N} = \frac{H_{c1}^{fo}(0) - H_{c1}^{fo}(T)}{4SJ^z} \sqrt{j_z(0)}. \tag{23}$$

We then pass to plane (b) in Fig. 3.

2. $\sqrt{j_{xy}(0)} + \sqrt{j_z(0)} < 1$

The phase diagram in this case is shown in Fig. 3*c*. The temperature T^{**} is found from the condition $\sqrt{j_{xy}(T^{**})} + \sqrt{j_z(T^{**})} = 1$, with the result

$$T^{**} = T_N \left(1 - \sqrt{j_{xy}(0)} - \sqrt{j_z(0)}\right). \tag{24}$$

At $T < T^{**}$, there are transitions from the spiral phase to the collinear one with all spins aligned along the field direction (phase III). In contrast, at $T > T^{**}$, there is first-order a transition to the collinear phase with $\theta \neq 0$ and then a second-order phase transition to phase III. The phase transition between the spiral and collinear phases is of the first and second order at $T < T^*$ and $T > T^*$, respectively, where T^* is given by Eq. (22).

4. CONCLUSIONS

We have discussed a nonfrustrated magnetoelectric with Hamiltonian (2) in the magnetic field with the spin–lattice coupling of form (1) assumed to be strong enough to produce the spiral spin structure inducing ferroelectricity. The ground-state energy was analyzed. We show that in contrast to the naive expectation, the onset of ferroelectricity occurs at $H < H_{c1}$, where H_{c1} is lower than the saturation field H_{c2} if the constant β in Eq. (1) is not too large. The type of the phase transition between the collinear paraelectric phase and the spiral ferroelectric phase depends on values of the constants j given by Eqs. (5): the transition is of the second order if condition (14) holds and of the first order if it does not hold. Moreover, if inequality (19) is not satisfied, there is only one critical field at which the first-order transition occurs from the spiral phase to the phase in which all spins are parallel to the field.

From a qualitative analysis using the mean-field approach, we obtained the phase diagram in the $H - T$ plane shown in Fig. 3. Increasing β corresponds to successively passing from plane (*a*) to (*b*) and (*c*). We also note that the phase diagram remains qualitatively the same for a magnetoelectric with the antiferromagnetic coupling among spins in the xy plane (cf. Eq. (2)). In contrast, if the exchange coupling along the z axis is ferromagnetic, the constant j_z should be set equal to zero in the above consideration. As a consequence, we obtain the phase diagram shown in Fig. 3*c*.

This work was supported by the Russian Science Support Foundation, the President of the Russian Federation (grant MK-4160.2006.2), the RFBR (grants 06-02-16702 and 06-02-81029), and Russian Programs "Quantum Macrophysics", "Strongly Correlated Electrons in Semiconductors, Metals, Superconductors and Magnetic Materials", and "Neutron Research of Solids".

REFERENCES

1. M. Fiebig, J. Phys. D: Appl. Phys. **38**, R123 (2005).
2. S.-W. Cheong and M. Mostovoy, Nature Mater. **6**, 13 (2007).
3. A. B. Harris and G. Lawes, E-print archives, cond-mat/0508617.
4. N. Aliouane, D. N. Argyriou, J. Strempfer, I. Zegkinoglou, S. Landsgesell, and M. v. Zimmermann, Phys. Rev. B **73**, 020102(R) (2006).
5. M. Kenzelmann, A. B. Harris, S. Jonas, C. Broholm, J. Schefer, S. B. Kim, C. L. Zhang, S.-W. Cheong, O. P. Vajk, and J. Lynn, Phys. Rev. Lett. **95**, 087206 (2005).
6. T. Kimura, G. Lawes, T. Goto, Y. Tokura, and A. P. Ramirez, Phys. Rev. B **71**, 224425 (2005).
7. N. Hur, S. Park, P. A. Sharma, J. S. Ahn, S. Guha, and S.-W. Cheong, Nature **429**, 392 (2004).
8. L. C. Chapon, P. G. Radaelli, G. R. Blake, S. Park, and S.-W. Cheong, Phys. Rev. Lett. **96**, 097601 (2006).
9. G. R. Blake, L. C. Chapon, P. G. Radaelli, S. Park, N. Hur, S.-W. Cheong, and J. Rodriguez-Carvajal, Phys. Rev. B **71**, 214402 (2005).
10. A. B. Harris, T. Yildirim, A. Aharony, and O. Entin-Wohlman, Phys. Rev. B **73**, 184433 (2006).

11. M. Kenzelmann, A. B. Harris, A. Aharony, O. Entin-Wohlman, T. Yildirim, Q. Huang, S. Park, G. Lawes, C. Broholm, N. Rogado et al., Phys. Rev. B **74**, 014429 (2006).

12. Y. Yamasaki, S. Miyasaka, Y. Kaneko, J.-P. He, T. Arima, and Y. Tokura, Phys. Rev. Lett. **96**, 207204 (2006).

13. K. Taniguchi, N. Abe, T. Takenobu, Y. Iwasa, and T. Arima, Phys. Rev. Lett. **97**, 097203 (2006).

14. T. Kimura, G. Lawes, and A. P. Ramirez, Phys. Rev. Lett. **94**, 137201 (2005).

15. A. B. Harris, E-print archives, cond-mat/0610241.

16. M. Mostovoy, Phys. Rev. Lett. **96**, 067601 (2006).

17. I. A. Sergienko and E. Dagotto, Phys. Rev. B **73**, 094434 (2006).

18. H. Katsura, N. Nagaosa, and A. V. Balatsky, Phys. Rev. Lett. **95**, 057205 (2005).

19. H. Katsura, A. V. Balatsky, and N. Nagaosa, Phys. Rev. Lett. **98**, 027203 (2007).